

# Flying-capacitor Linear Amplifier for Wireless Power Transfer Systems with Flying-capacitor Voltage Balancing

Rintaro Kusui, Keisuke Kusaka, Jun-ichi Itoh  
Nagaoka University of Technology  
1603-1, Kamitomioka Nagaoka  
Niigata, Japan

Tel.: +81 / (258) – 46.9622

Fax: +81 / (258) – 46.9622

E-Mail: kusui@stn.nagaokaut.ac.jp, kusaka@vos.nagaokaut.ac.jp, itoh@vos.nagaokaut.ac.jp

URL: <http://itohserver01.nagaokaut.ac.jp/itohlab/en/index.html>

## Keywords

Amplifiers, Capacitor voltage balancing, Flying Capacitor Converter, Wireless power transmission

## Abstract

In this paper, a flying-capacitor linear amplifier (FCLA) for wireless power transfer systems is proposed. The proposed circuit has an  $n$ -series FCLA with only N-ch MOSFETs and an unfolders. The flying capacitor (FC) voltages are balanced by selecting the operation state of each MOSFET with phase-shifted carriers. FCLA outputs a continuous voltage that does not contain the harmonics that cause current harmonics. Due to this, the radiation noise from the transmission coils is reduced. The operation of the WPT system with the proposed 16-series FCLA is demonstrated in a simulation. The proposed FCLA output the sinusoidal voltage to the resonance circuit. In addition, the harmonics of the primary coil current are analyzed. From this result, the FCLA significantly reduces the current harmonics than the conventional two-level inverter. Then, The FC voltage balance is verified using the prototype with a 2-series FCLA. From the experimental results with a small-scale prototype, the proposed circuit outputs full-wave rectified sinusoidal output voltage with balanced FC. Furthermore, the harmonics of the unfolders output voltage are analyzed. From the analyzed result, the third-order harmonics are reduced by 19.8dB due to FCLA with MOSFET in the active-state in comparison with the theoretical value of harmonics of square wave voltage.

## Introduction

In recent years, wireless power transfer (WPT) systems are actively studied for electric vehicles (EVs)<sup>[1-5]</sup>. The WPT system may improve user convenience due to power transmission without connecting cables. However, the WPT system generates radiation noise from transmission coils because the WPT system transmits power through weak magnetic coupling between two coils. The radiation noise may cause malfunction of electric devices and interference of wireless communication. For this reason, the International special committee on radio interference (CISPR: Comité International Spécial des Perturbations Radioélectriques) has published reference levels of radiation noise<sup>[6]</sup>. Moreover, the regulation of CISPR for electromagnetic field emission from WPT systems, especially for harmonic components of electromagnetic fields (EMF), is planning to be tightened significantly<sup>[7]</sup>. Accordingly, the WPT system must reduce the radiation noise.

In conventional WPT systems, the inverter that outputs square wave voltage is used for the primary side power supply<sup>[8]</sup>. The current contains low-order harmonics flowing on transmission coils due to applying the square wave voltage with low-order harmonics to the resonance circuit and transmission coils. Thus, the radiation noise is generated around the transmission coil not only at the fundamental component but also at the low-order harmonics.

In [9-11], metal plates, magnetic materials, and additional windings shield the radiation noise from the WPT system. The shield reduces the radiation noise by flowing the current on the shield. Due to this, the eddy current loss occurs by the current through the shield. Improvement of the shield performance and cooling cause increasing in the volume of the shield. Ref. [12-14] propose the three-phase WPT system with 12-coils. The pair of coils on each phase connected in series in a differential connection canceled out the radiation noise. A three-phase WPT system with 12 coils complies with the current guidelines; however, it is not enough to comply with generation guidelines.

In this paper, a flying-capacitor linear amplifier (FCLA) for WPT systems is proposed. The proposed FCLA outputs sinusoidal voltage without PWM. The sinusoidal voltage without PWM reduces the current harmonics on the coils. In other words, the radiation noise from the WPT system will be reduced by the proposed FCLA. However, output voltage distortion occurs by P-ch MOSFETs used in the conventional FCLA [15-16]. In the proposed FCLA, P-ch MOSFETs are removed using an unfold. In addition, flying capacitor (FC) voltages are automatically balanced by selecting the operation states of the MOSFETs by comparing asynchronous phase-shifted carriers. The originality of this paper is proposing an FCLA without p-ch MOSFET, which has the self-balancing capability of the FC voltage. The proposed FCLA for WPT is demonstrated in this paper. It is confirmed that the FC voltage balance by the prototype.

## Flying-capacitor linear amplifier for wireless power transfer

### System configuration

Figure 1 shows the static characteristics of an N-ch MOSFET. The operation states are divided into ON, OFF, and active states depending on the drain-source and gate-source voltages. Traditional switching power converters use only the ON and OFF states. The high-frequency leakage current generates high-order components of the radiation noise. Besides, FCLA outputs a continuous voltage using one of the series-connected MOSFETs in the active state. The conventional FCLA needs complementary MOSFETs [4-7]. One of the N-ch MOSFETs is in the active state when the FCLA output the positive current. On the other hand, the P-ch MOSFET is in the active state when the FCLA output the negative current. In the conventional FCLA, the P-ch MOSFETs decrease efficiency due to their higher conduction loss and switching loss than the N-ch MOSFETs.

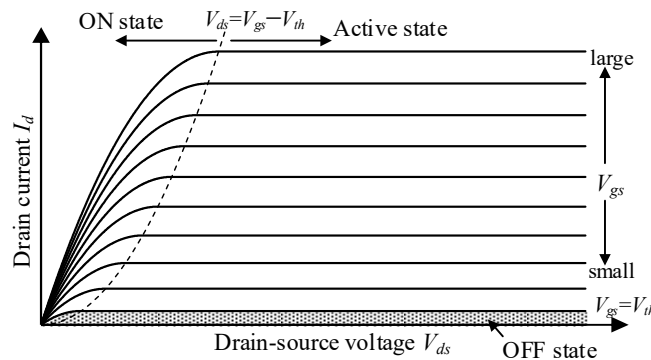


Fig. 1. Operation state of N-ch MOSFET.

Figure 2 shows the system configuration of the WPT system with the proposed FCLA. The proposed circuit has an  $n$ -series FCLA with  $n$  N-ch MOSFETs and  $n$  diodes connected in series and an unfold. The proposed FCLA outputs a full-wave rectified voltage. The unfold outputs a sinusoidal voltage by switching the polarity of the FCLA output voltage. Meanwhile, the WPT is operated in a unity power factor, i.e., the voltage and the current are in phase. For these reasons, in the proposed FCLA, only N-ch MOSFETs are used in the active state for output voltage control. Therefore, the P-ch MOSFETs can be replaced by diodes.

An isolated gate drive unit (GDU) is connected to each MOSFET. The GDU adds the DC bias to gate-source voltage to control the state of MOSFET. The current path of FCLA depends on

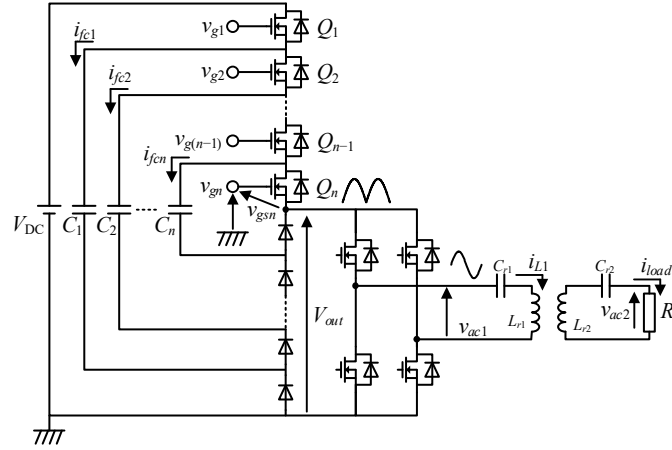


Fig. 2. FCLA with the unfold for WPT.

the combination of MOSFET states. The charge or discharge of FCs is switched by the current path. Accordingly, the flying capacitor (FC) voltages are balanced by the appropriate selection of each MOSFET state.

### State selection for MOSFET

Figure 3 shows a method for selecting the operation state of each MOSFET in a 4-series FCLA using phase-shifted carrier comparison. The state selection to FC voltage balancing is complicated because of enormous flexibility in the current paths of FCLA. The state is selected by the phase-shifted carriers comparison using conventional flying capacitor converter in the proposed system. The phase-shifted carriers are compared with the stepped thresholds value to select the state of MOSFET from ON, OFF, and active states. The thresholds depend on the output voltage command. The output voltage range of FCLA is change by the number of the MOSFET in the OFF state. Assuming balanced FC voltages, the output voltage range of the  $n$ -series FCLA when  $k$  N-ch MOSFETs are operating in the OFF state is expressed as

$$\frac{n-k-1}{n}V_{DC} < v_{out} \leq \frac{n-k}{n}V_{DC} \quad (1).$$

Accordingly, the threshold to select off state is stepped value changed by  $1/n$  depended on output command. The threshold to select ON state is  $1/n$  smaller than the threshold to select OFF state. The ON state is selected when the carrier is smaller than the threshold for the ON state, and the OFF state is selected when the carrier is larger than the threshold for the OFF state. Furthermore, the MOSFET, which is not selected ON or OFF state, is an active state. The carrier frequency is set close to the output frequency to avoid changing the state redundancy. When the carrier frequency is synchronized with the output frequency, the same current path is selected for each cycle. Due to this, the FC voltage is imbalanced because the integral of the FC current does not equal zero. On the other hand, the integral

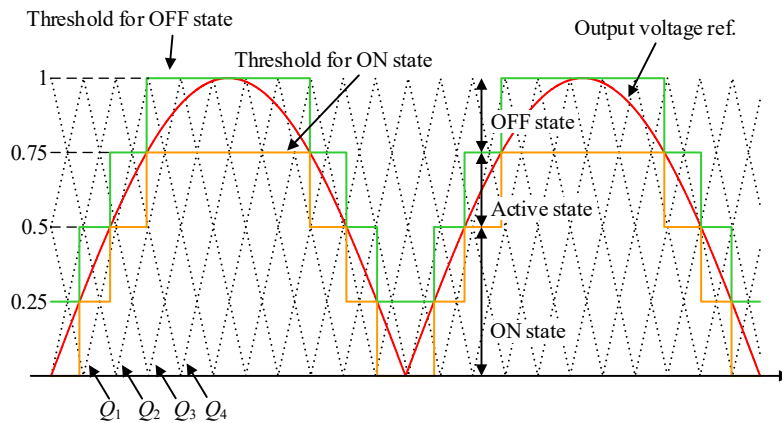


Fig. 3. State selection by comparing with phase-shifted carrier for 4-series FCLA.

of the FC current becomes zero in a few cycles because the different current path is selected in each period when the asynchronous carrier is used. In other words, the FC voltages keep balancing by using asynchronous carriers to select the operation state.

### Output voltage control

Figure 4 shows a block diagram of the FCLA voltage controller. In the proposed system, the output voltage is controlled by proportional control. The operation state of each MOSFET is controlled by adding a DC bias depending on the selected state. Moreover, the controller changes the states to balance the FC voltages when the FC voltages are imbalanced. The output voltage  $V_{out}$  of the FCLA is expressed as

$$V_{out} = \frac{V_{DC}}{n} \sum_{i=1}^n S_i + \sum_{k=1}^{n-1} \Delta V_{fci} (S_{i+1} - S_i) \quad (2),$$

where  $S_i$  is the state of the  $i$ -th MOSFET, and represents the OFF state as “0”, the ON state as “1”, and the active state as  $0 < S_i < 1$ . The second term of (2) shows the effect of the error  $\Delta V_{fci}$  of the FC voltage on the output voltage. From (2), the FC voltages imbalance changes the output voltage range. Due to this, it is impossible to output the voltage in the reduced range by FC voltage imbalance. Then, the voltage controller increases or decreases the gate-source voltage  $v_{gsk}$  to transition the operation point of MOSFET.

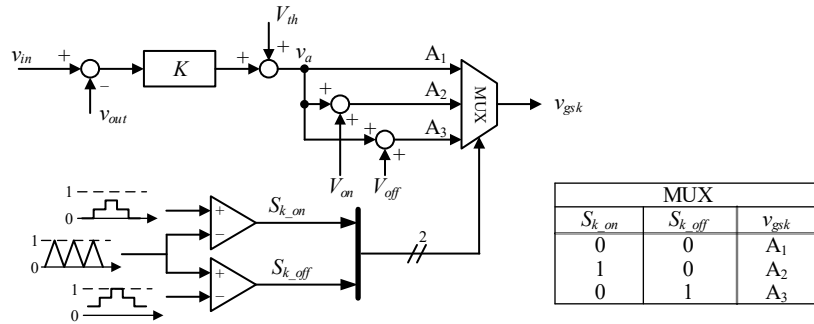


Fig. 4. Voltage control diagram.

Figure 5 shows the current paths in each pattern of the operation state of the two-series FCLA. A two-series FCLA has four patterns because one of the MOSFETs connected in series operates in the active state. The FCs in  $n$ -series FCLA are charged or discharged in the current paths which one or more MOSFETs are in OFF state. In two-series FCLA, the FC is charged or discharged in the current path (a) and (c). The FC voltage is balanced when the integral of the FC current in the current path (a) is equal to it in the current path (c). Similarly, the FC voltages in the  $n$ -series FCLA are balanced when the integral of FC current is zero. However, when the FC voltage is imbalanced, the current path must be changed to compensate for the error from the nominal FC voltage.

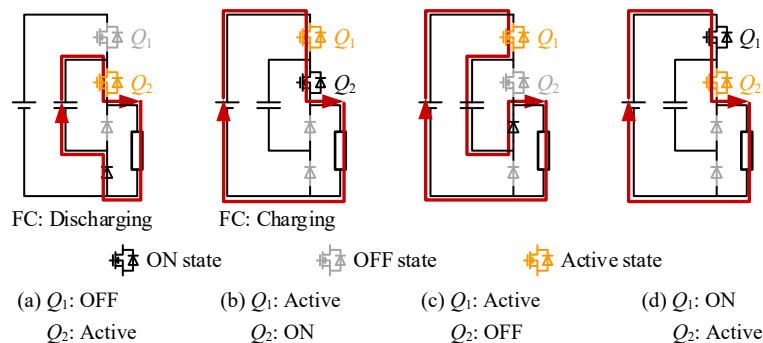


Fig. 5. Current path of 2-series FCLA.

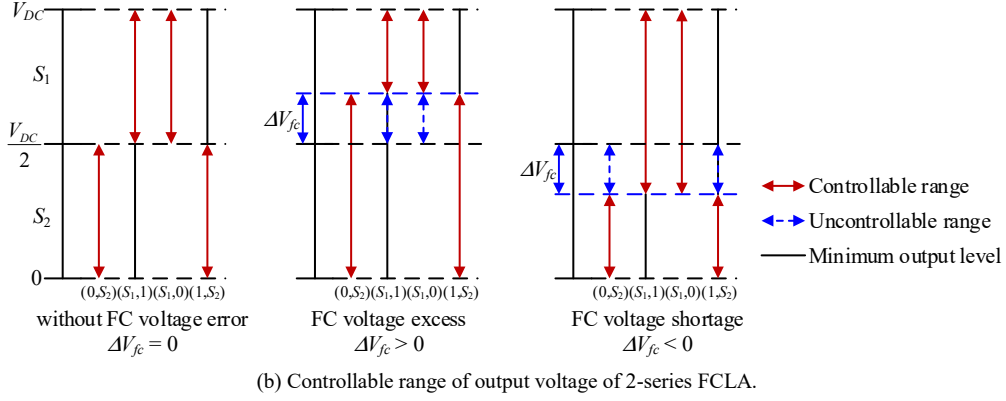
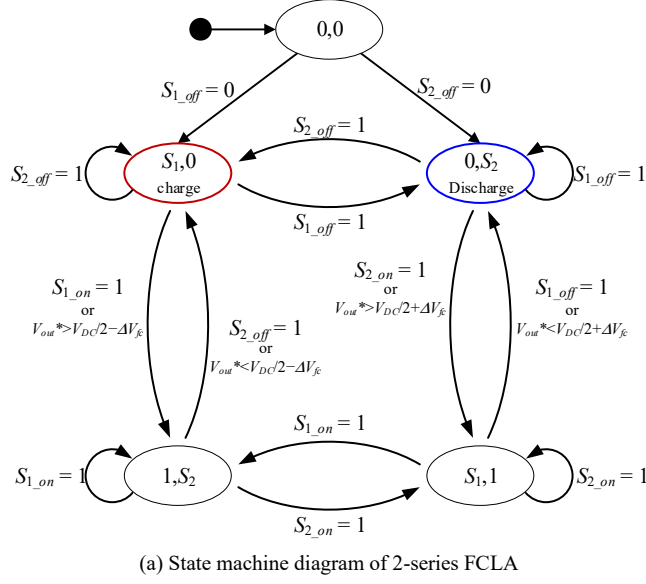


Fig. 6. Automatically self-balancing capability for FC voltage in two-series FCLA

Fig. 6 (a) shows the state-machine diagram and (b) shows the controllable voltage range for each of the selected states in a two-series FCLA. The state of two MOSFETs is represented as  $(S_1, S_2)$ , where OFF state is represented as “0”, the ON state is represented as “1”, and the active state is represented as  $S_1$  or  $S_2$ . In Fig. 6 (b), the red arrows are the range of controllable voltages, and the black line is the minimum output voltage for each pattern. The sum of the red arrow and the black line is the maximum voltage. When the FC voltages are balanced, the transition of the state is caused by carrier comparison and not by the voltage controller. The voltage controller changes the state when the output voltage range is reduced by the FC voltage imbalance. The controllable range of output voltage with imbalance FCs is expressed as

$$\frac{n-k-1}{n}V_{DC} + \Delta V_{fci} (S_{i+1} - S_i) < V_{out} \leq \frac{n-k}{n}V_{DC} + \Delta V_{fci} (S_{i+1} - S_i) \quad (3),$$

where  $\Delta V_{fci}$  is the voltage error of  $i$ -th FC voltage from nominal value and  $k$  is the number of MOSFETs in OFF state. From (3), the voltage range of the two-series FCLA in the state of  $S_1$  in the active state is reduced when the FC voltage excess half of the DC voltage, i.e., the voltage error is positive. Due to this, the state of FC not discharging changes the state of FC discharging, and the state of FC charging changes one of FC charging. Besides, the voltage range is reduced when the state of  $S_2$  is active and the FC voltage error is negative. Because of this, the voltage controller reduces the discharging period and increases the charging period. For these results, the voltage controller automatically compensates the imbalance of FC voltage. Similarly, the FC voltages in  $n$ -series FCLA are automatically balanced by carrier comparison and voltage controller.

Table 1. Simulation condition

Parameters	Symbol	Value
Primary voltage	$V_{DC1}$	650 V
Secondary voltage	$v_{out}$	460 V
Output power	$P$	30 kW
Transmission frequency	$f$	85 kHz
Coupling Coefficient	$k$	0.3
Primary inductance	$L_1$	43.9 $\mu$ H
Secondary inductance	$L_2$	27.0 $\mu$ H
Primary capacitance	$C_{r1}$	79.8 nF
Secondary capacitance	$C_{r2}$	130 nF
Number of series	$n$	16
Flying capacitance	$C_k$	10 $\mu$ F

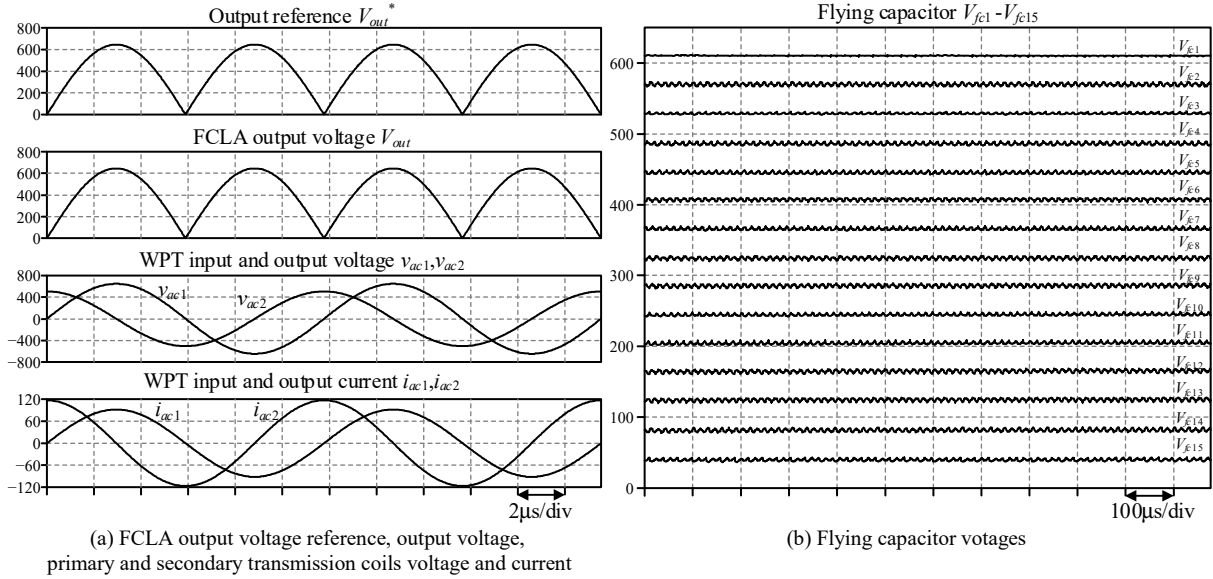


Fig. 7. Simulataion waveforms of 16-series FCLA and WPT system

## Simulation of the WPT system with proposed FCLA

### Operation waveform

Figure 7 shows simulation waveforms of the WPT system with 16-series proposed FCLA and table 1 shows the simulation conditions. The simulations are used the MOSFET model for the SPICE simulator provided by the MOSFET manufacturers. Fig. 7 (a) shows the FCLA output voltage command, output voltage, and the voltage and current waveforms on the primary and secondary sides of the transmission coil. Figure 7 (b) shows the FC voltages waveforms. From Fig. 7 (a), it is confirmed that the output voltage of FCLA follows the command. In addition, it is confirmed that the proposed FCLA applies a sinusoidal voltage to the transmission coil and operates the WPT in resonant conditions. From Fig. 7 (b), it is confirmed that the FC voltages are balanced by selecting the operation state of the MOSFETs using the phase-shifted carriers.

Figure 8 shows the simulation waveforms at the start-up of 4-series FCLA with zero-voltage FCs. In this simulation, the DC voltage is 160V. From Fig. 8, it is seen that the FC voltages converge at nominal value in the steady-state. From this result, it is confirmed that the voltage controller has the capability of automatically balancing for the FC voltages.

### Analysis of coil current harmonics

Figure 9 shows the harmonics analysis results of the current on the primary coil in the WPT system because the radiation noise from the WPT system is proportional to coil current. The current harmonics are analyzed with 16-series FCLA, 17-level flying capacitor converter (FCC), and two-level inverter as

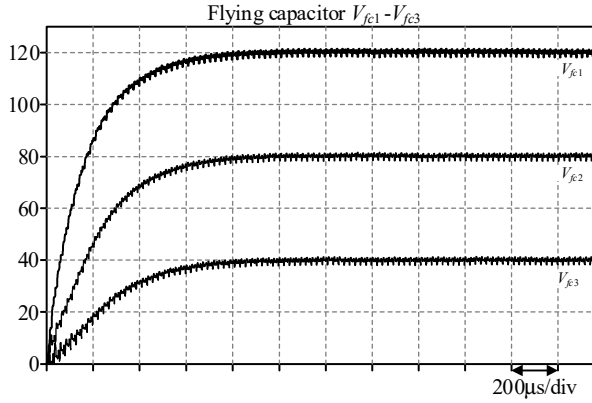


Fig. 8. FC voltage balancing capability in 4-series FCLA

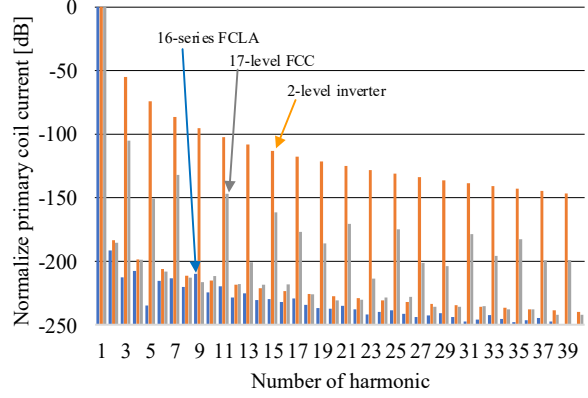


Fig. 9. Harmonic analysis for primary coil current

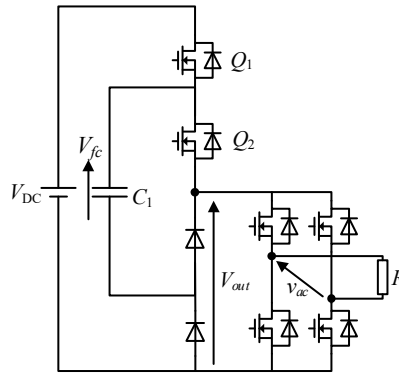


Fig.10. Circuit configuration of prototype.

the power supply in the WPT system, respectively. In addition, each analysis result is normalized based on the fundamental frequency component. From Fig. 9, the current harmonics are significantly reduced by using the FCC or FCLA. Focusing on the third harmonics components, the 17-level FCC reduces the current harmonics by 50dB, and the 16-series FCLA reduced it by more than 100dB in comparison with using the inverter.

## Evaluation of FC voltage balance with two-series FCLA

Figure 10 shows the configuration of the prototype to verify the FC voltage balance. The prototype has a two-series FCLA and an unfolder. The MOSFET for the FCLA should be 60-V breakdown voltage and low on-resistance for efficiency and availability. For this reason, the DC voltage is 80 V so that the applied voltage of one MOSFET is about 40 V. The load  $R$  is 100  $\Omega$ , and the output voltage command  $V_{out}^*$  is a full-wave rectified voltage with an amplitude of 80 V and a frequency of 50 Hz for the demonstration of the voltage balance.

Figure 11 (a) shows the operation waveforms of two-series FCLA, and Fig. 11 (b) shows the enlarged waveform of fig.11(a). From Fig. 11(a), the average FC voltage is 40 V, which is half of DC voltage. In other words, the FC voltage is balanced by carrier comparison. From Fig. 11(b), the FCLA outputs the full-wave rectified voltage following to command value. Furthermore, the unfolder switches the polarity of FCLA output voltage and outputs sinusoidal voltage. However, the distortion of FCLA output voltage occurs by the nonlinearity of MOSFET and the time delay on the analog isolation amplifier in the voltage controller.

Figure 12 shows the operation waveform at the start-up of the 2-series FCLA. The FC voltage is 0 V in the initial condition, i.e., the FC voltage is imbalanced. From Fig. 12, the FC voltage is converged at a nominal value. Accordingly, it is confirmed the automatically self-balancing capability of the voltage controller.

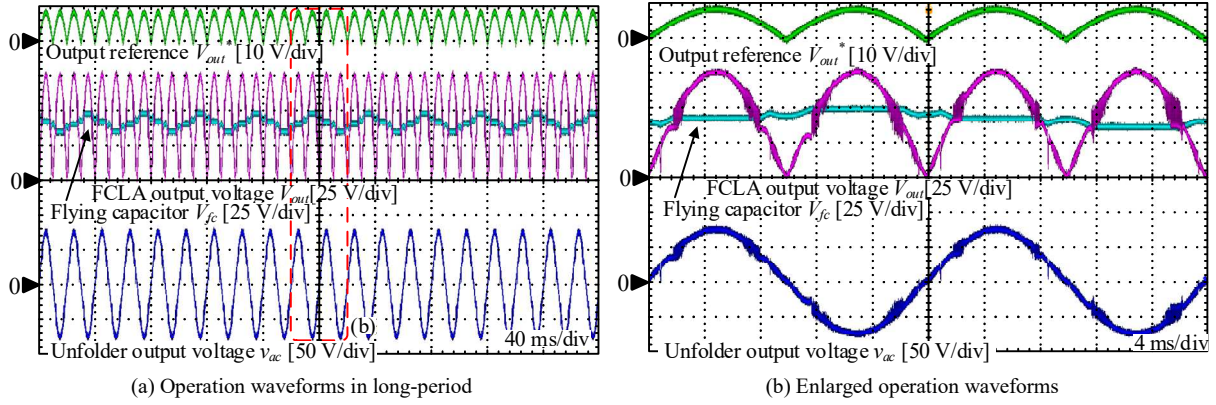


Fig. 11. Operation waveforms of 2-series FCLA.

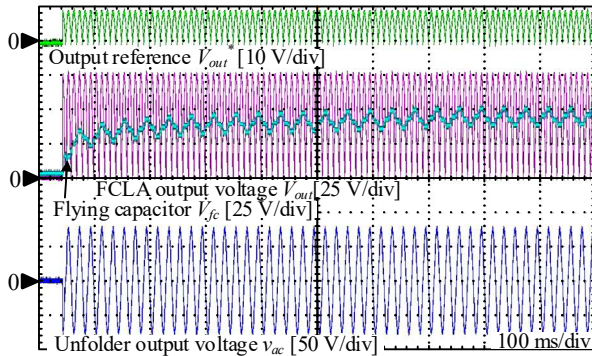


Fig. 12. Start-up of the 2-series FCLA

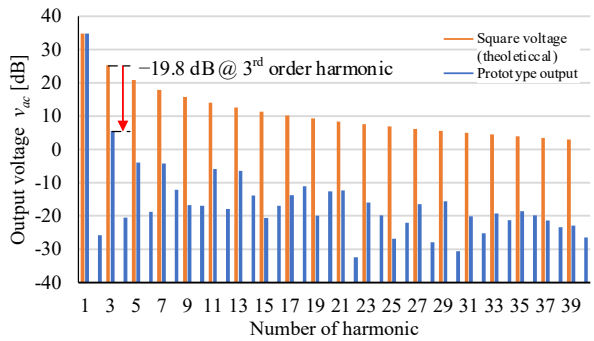


Fig. 13. Harmonic analysis of unfold output voltage.

Figure 13 shows the harmonics analysis results of prototype output voltage. The voltage harmonic is evaluated because the load is pure resistance load. In addition, Fig. 13 shows the theoretical value of harmonics of the square voltage whose fundamental components are equal to the prototype output voltage. From the analysis results, the odd-order harmonics are reduced by 15dB or more than square voltage. Focusing on the third harmonic, the FCLA reduces the voltage harmonic by 19.8dB.

## Conclusion

This paper proposed the FCLA with only N-ch MOSFET to reduce the radiation noise harmonics from the WPT system. The proposed circuit has an  $n$ -series FCLA and an unfolder. The FCLA outputs a sinusoidal voltage without harmonics by operating one of the MOSFETs in the active state. The operation state of each MOSFET is selected by comparing with phase-shift carriers to keep balancing the FC voltages. In addition, the output voltage is controlled by output voltage feedback. The selection by phase-shifted carries and controller balances the FC voltages. From this result, the proposed FCLA reduces the current harmonics in comparison with using the conventional two-level inverter by applying the continuous sinusoidal voltage to the resonance circuit. Then, The balancing of the FC voltage by the carrier comparison and the voltage controller is verified with the 2-series FCLA. From the experimental results, it is confirmed that the FCLA outputs voltage following the command while the FC voltage is balanced. In addition, the harmonic of the unfold output voltage is analyzed. The third-order harmonic is reduced by 19.8dB than the theoretical value of square voltage.

## References

- [1] T. Diekhans and R. W. De Doncker: "A Dual-Side Controlled Inductive Power Transfer System Optimized for Large Coupling Factor Variations and Partial Load", IEEE Trans. on Power Electronics, Vol. 30, No. 11, pp. 6320-6328 (2015)
- [2] A. Tejada, S. Kim, F. Y. Lin, G. A. Covic and J. T. Boys: "A Hybrid Solenoid Coupler for Wireless Charging Applications," IEEE Trans. on Power Electronics, vol. 34, no. 6, pp. 5632-5645 (2019)

- [3] G. Lovison, T. Imura, H. Fujimoto, Y. Hori: "Secondary-side-only Phase-shifting Voltage Stabilization Control with a Single Converter for WPT Systems with Constant Power Load", IEEJ Journal of Industry Applications, Vol. 8, No. 1, pp. 66-74 (2019)
- [4] R. Ota, N. Hoshi, J. Haruna: "Design of Compensation Capacitor in S/P Topology of Inductive Power Transfer System with Buck or Boost Converter on Secondary Side", IEEJ Journal of Industry Applications, Vol. 4, No. 4, pp. 476-485 (2015)
- [5] M. Budhia, J. T. Boys, G. A. Covic, C. Huang: "Development of a Single-Sided Flux Magnetic Coupler for Electric Vehicle IPT Charging Systems," IEEE Tran. on Industrial Electronics, Vol. 60, No. 1, pp. 318-328, (2013)
- [6] Ministry of Internal Affairs and Communications, Japan, "Inquiry of technical requirements for wireless power transfer system for EVs in technical requirements for wireless power transfer system in standards of International Special Committee on Radio Interference (CISPR)", (2015)
- [7] N. Misawa : " Situation of EMC Limit Level of WPT for EV in CISPR", 2019 JSAE Annual Congress (Spring) Latest Trend of EV Charging System, No. 20194438, pp.15-20 (2019)
- [8] K. Kusaka, J. Itoh: "Development Trends of Inductive Power Transfer Systems Utilizing Electromagnetic Induction with Focus on Transmission Frequency and Transmission Power," IEEJ Journal of Industry Applications, Vol. 6, No. 5, pp. 328-339 (2017)
- [9] Keita Furukawa, Keisuke Kusaka, Jun-ichi: "EMF Reduction with Compensated Current RMS Based on Short Canceling Coils for Wireless Power Transfer Systems", IEEJ Trans. on Industry Applications, Vol. 141, No. 5, pp. 405-415 (2021)
- [10] M. Mohammad, S. Choi: "Optimization of ferrite core to reduce the core loss in double-D pad of wireless charging system for electric vehicles," 2018 IEEE Applied Power Electronics Conference and Exposition (APEC), pp. 1350-1356 (2018)
- [11] H. Moon, S. Kim, H. H. Park, S. Ahn, "Design of a Resonant Reactive Shield With Double Coils and a Phase Shifter for Wireless Charging of Electric Vehicles," IEEE Tran. on Magnetics, Vol. 51, No. 3, pp. 1-4, (2015)
- [12] Keisuke Kusaka, Keita Furukawa, Jun-ichi Itoh, Development of Three-Phase Wireless Power Transfer System with Reduced Radiation Noise, IEEJ Journal of Industry Applications, 2019
- [13] K. Kusaka, R. Kusui, J. Itoh, D. Sato, S. Obayashi, M. Ishida: "A 22 kW-85 kHz Three-phase Wireless Power Transfer System with 12 coils," 2019 IEEE Energy Conversion Congress and Exposition (ECCE), pp. 3340-3347, (2019)
- [14] R. Kusui, K. Kusaka, J. Itoh, S. Obayashi, T. Shijo M. Ishida: "Downsizing of Three-Phase Wireless Power Transfer System with 12 coils by Reducing Magnetic Interference," 2020 IEEE 29th International Symposium on Industrial Electronics (ISIE), pp. 1442-1447 (2020)
- [15] H. Fujita, N. Yamashita, "Performance of a Diode-Clamped Linear Amplifier," IEEE Tran. on Power Electronics, Vol. 23, No. 2, pp. 824-831 (2008)
- [16] Hidemine Obara, Tatsuki Ohno, Masaya Katayama, Atsuo Kawamura: "Flying-Capacitor Linear Amplifier with Capacitor Voltage Balancing for High-Efficiency and Low Distortion", IEEE Trans. on Industry Applications, Vol.57, No.1 (2021)